Supplementary Materials

Selective photooxidation of 5-hydroxymethylfurfural in water enabled by highly dispersed gold nanoparticles on graphitic carbon nitride

Qizhao Zhang[1], Botao Fan[1], Yuxi Wang[1], Bang Gu[1,*], Qinghu Tang[2], Feng Qiu[3], Qiue Cao[1], Wenhao Fang[1,*]

[1]School of Chemical Science and Technology, Yunnan University, Kunming 650091, Yunnan, China.
[2]School of Chemistry and Chemical Engineering, Collaborative Innovation Center of Henan Province for Green Manufacturing of Fine Chemicals, Key Laboratory of Green Chemical Media and Reactions - Ministry of Education, Henan Normal University, Xinxiang 453007, Henan, China.
[3]National Center for International Research on Photoelectric and Energy Materials, School of Materials and Energy, Yunnan University, Kunming 650091, Yunnan, China.

[*]**Correspondence to:** Dr. Bang Gu and Prof. Wenhao Fang, School of Chemical Science and Technology, Yunnan University, 2 North Cuihu Road, Kunming 650091, Yunnan, China. E-mail: gubang@ynu.edu.cn; wenhao.fang@ynu.edu.cn

Supplementary Table 1. The precise Au loading measured by ICP-MS and the mean Au size calculated by the Scherrer equation

Catalyst	Au loading (wt%)	(h k l)	2θ (°)	FWHM (°)	*d*, Au (nm)
Au/CN(I)	0.99	–	–	–	–
Au/CN(II)	1.02	(1 1 1)	38.2	1.252	6.7
Au/CN(III)	1.00	(1 1 1)	38.2	1.129	7.5

Supplementary Table 2. Comparison of catalytic performances of metal oxide-based catalysts for photooxidation of·HMF·to·DFF in water under simulated sunlight

Catalyst	Prod. DFF ($mg\ g^{-1}\ h^{-1}$)	Conv. HMF (%)	Select. DFF (%)	Yield DFF (%)	References
N/TiO_2	1.4	40	26	10	[1]
ZnO/PPy	3.1	5	12	1	[2]
$Au_3Cu_1/Ti_{15}Si_{85}$ SFD	4.5	21	34	7	[3]
Bi_2WO_6	19.2	26	73	19	[4]
HP brookite (TiO_2)	53	20	21	4	[5]
$(Cu_2O)_{0.16}\|TiO_2$	64.1	52	44	23	[6]
Au/CN(I)	72.7	68	38	26	This work

Supplementary Table 3. Energy band positions and band gaps of *g*-C_3N_4 carriers and supported-Au catalysts

Sample	E_g (eV)	$E_{VB'}$ *vs.* E_f (eV)	E_f *vs.* SCE (V)	E_f *vs.* NHE (V)	E_{VB} *vs.* NHE (V)	E_{CB} *vs.* NHE (V)	$E_{g\text{-}Au}$ (eV)	$E_{CB\text{-}Au}$ *vs.* NHE (V)
CN(I)	2.90	2.40	-0.80	-0.56	1.84	-1.06	–	–
CN(II)	2.87	2.30	-0.87	-0.63	1.67	-1.20	–	–
CN(III)	2.82	2.50	-0.91	-0.67	1.83	-0.99	–	–
ACN(I)	2.75	2.00	-0.98	-0.74	1.26	-1.49	1.51	-2.25
ACN(II)	2.74	1.10	-0.91	-0.67	0.43	-2.31	1.35	-2.02
ACN(III)	2.77	0.70	-0.92	-0.68	0.02	-2.75	1.25	-1.93

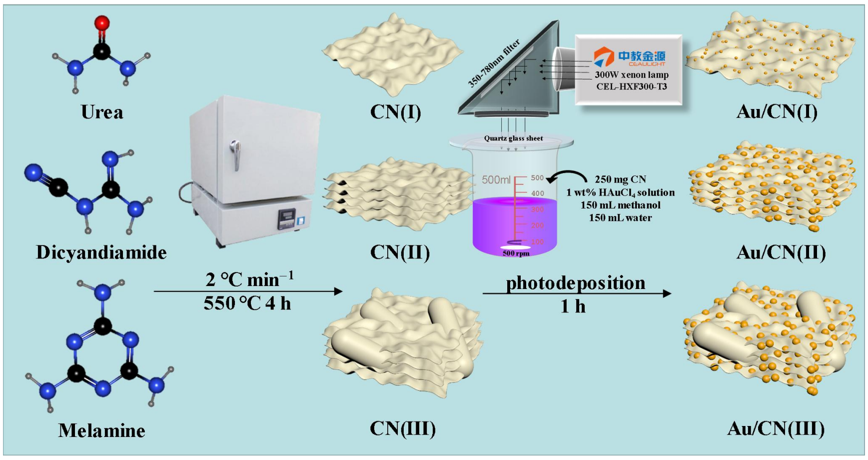

Supplementary Scheme 1. Schematic diagram for the photodeposition synthesis of *g*-C_3N_4 (*i.e.*, using three different precursors) supported-Au catalysts.

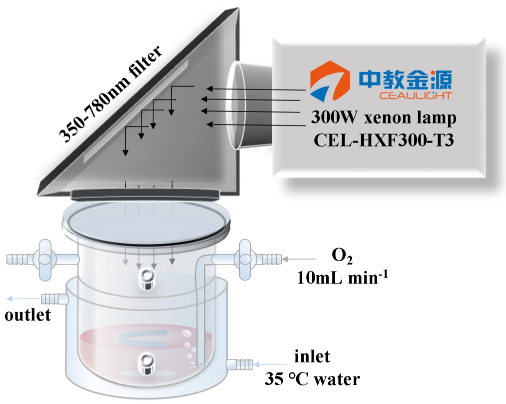

Supplementary Scheme 2. Schematic illustration of the photocatalytic reaction system.

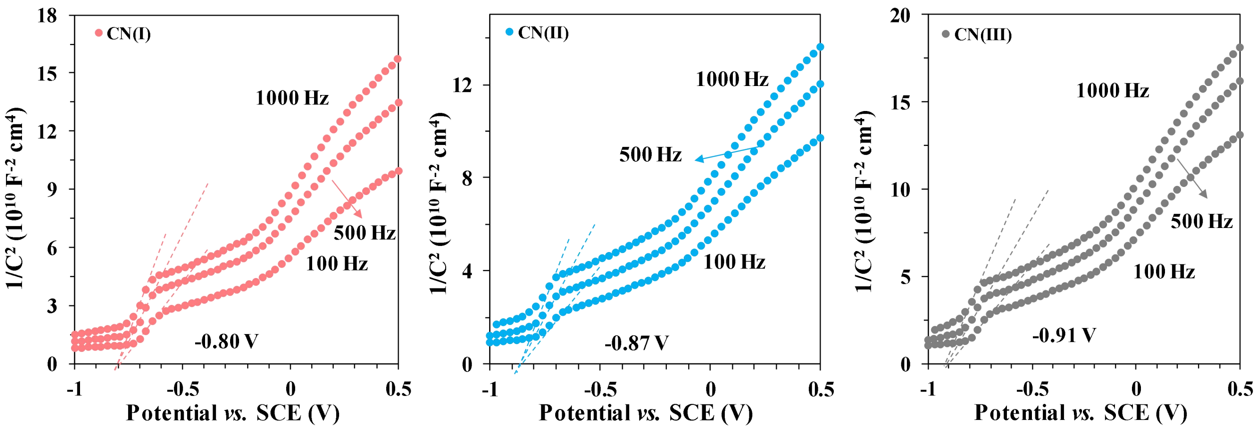

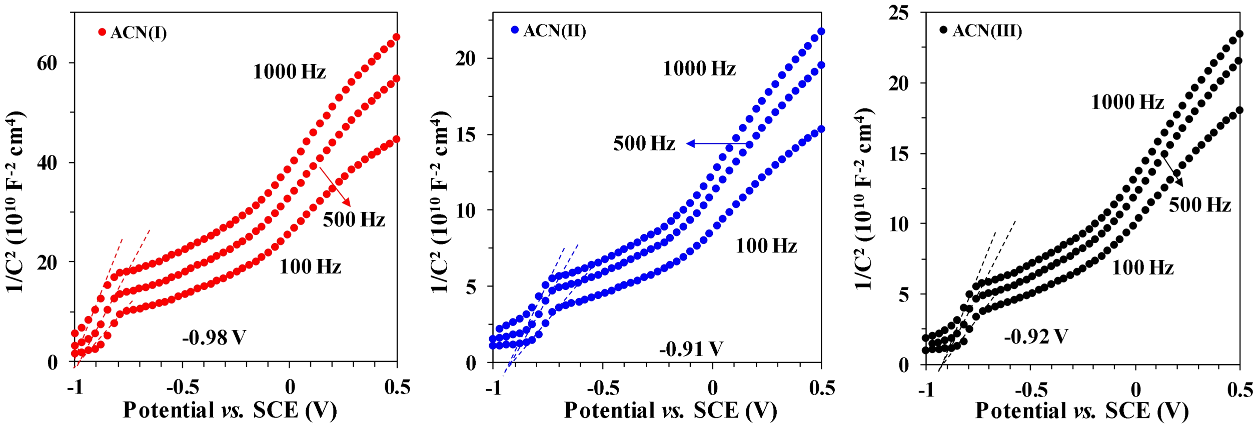

Supplementary Figure 1. Mott-Schottky plots of CN(I), CN(II), CN(III) Au/CN(I), Au/CN(II) and Au/CN(III).

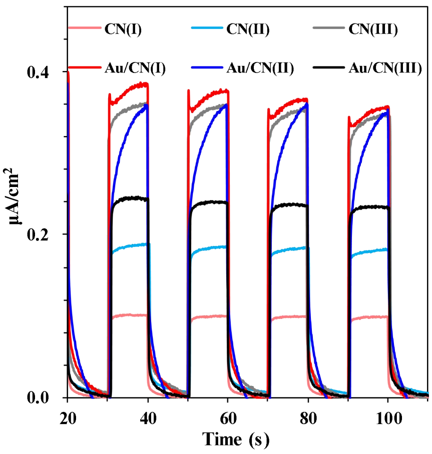

Supplementary Figure 2. Photocurrent measurement of *g*-C_3N_4 carriers and supported Au catalysts.

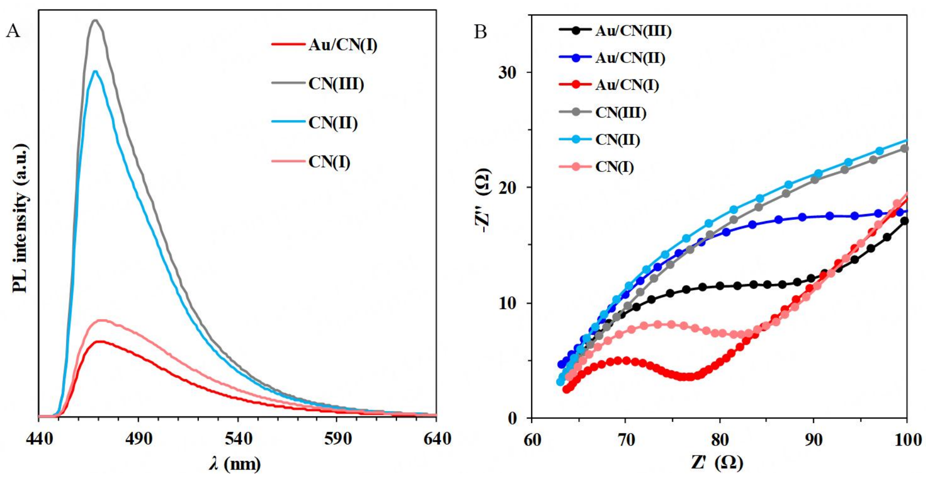

Supplementary Figure 3. (A) PL spectra of CN(I), CN(II), CN(III) and Au/CN(I); (B) EIS in the form of Nyquist plots of CN(I), CN(II), CN(III) Au/CN(I), Au/CN(II), and Au/CN(III).

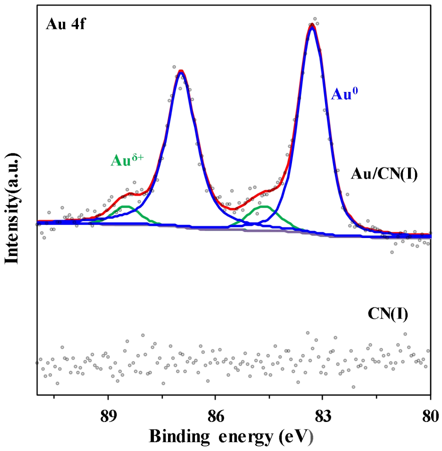

Supplementary Figure 4. XPS spectra of Au 4f core level for CN(I) and Au/CN(I).

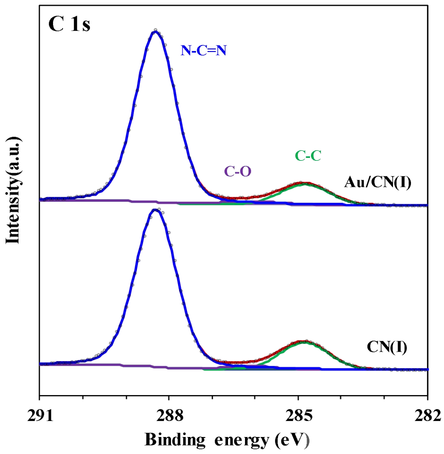

Supplementary Figure 5. XPS spectra of C 1s core level for CN(I) and Au/CN(I).

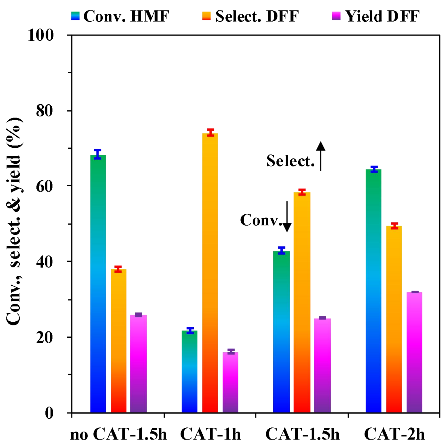

Supplementary Figure 6. Catalytic results of the controlled experiments over the Au/CN(I) catalyst by adding catalase scavenger for H_2O_2 during photooxidation of HMF to DFF.

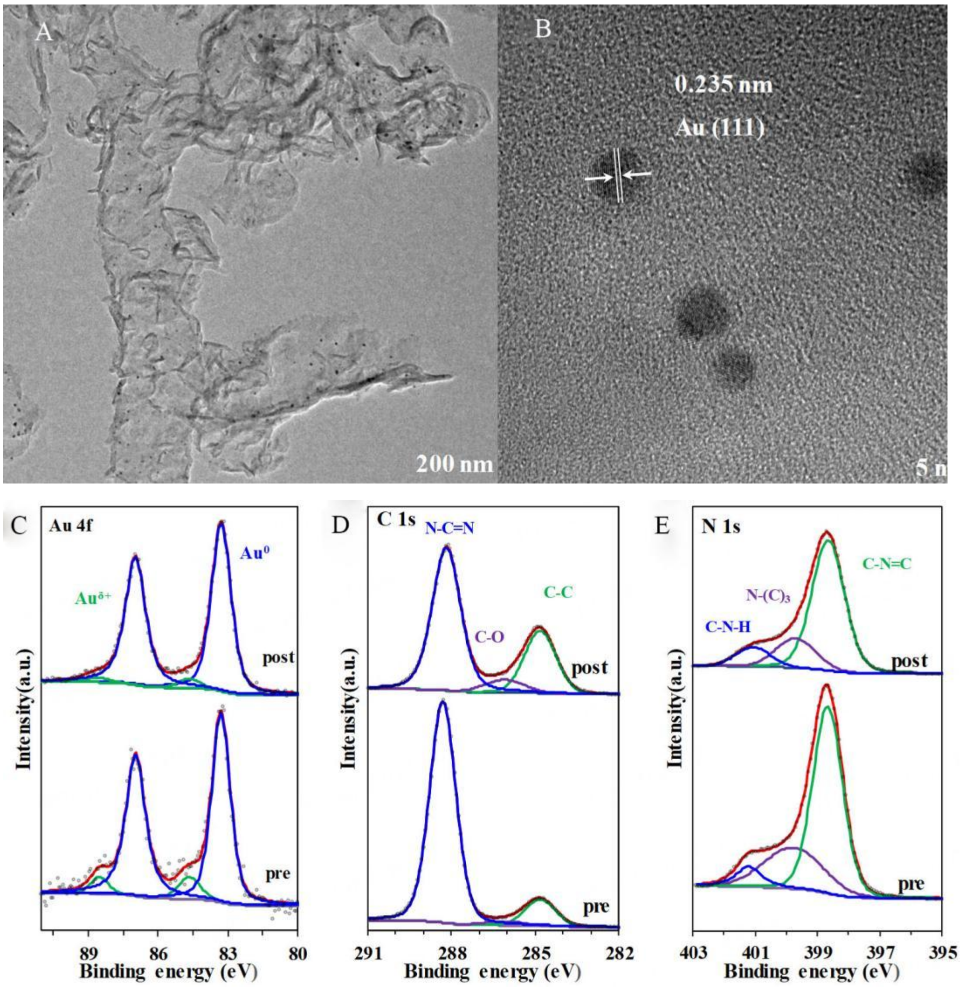

Supplementary Figure 7. (A) TEM and (B) HRTEM images, and (C-E) XPS spectra of the Au/CN(I) catalyst pre- and post-reaction.

References

1. Krivtsov I, Ilkaeva M, Salas-Colera E, et al. Consequences of Nitrogen Doping and Oxygen Enrichment on Titanium Local Order and Photocatalytic Performance of TiO_2 Anatase. *J Phys Chem C* 2017;121:6770-80. DOI: 10.1021/acs.jpcc.7b00354.
2. Gonzalez-Casamachin DA, Rivera De la Rosa J, Lucio–Ortiz CJ, Sandoval-Rangel L, García CD. Partial oxidation of 5-hydroxymethylfurfural to 2,5-furandicarboxylic acid using O_2 and a photocatalyst of a composite of ZnO/PPy under visible-light: Electrochemical characterization and kinetic analysis. *Chem Eng J* 2020;393:124699. DOI: 10.1016/j.cej.2020.124699.
3. Allegri A, Maslova V, Blosi M, et al. Photocatalytic Oxidation of HMF under Solar Irradiation: Coupling of Microemulsion and Lyophilization to Obtain Innovative TiO_2-Based Materials. *Molecules* 2020;25:5225. DOI: 10.3390/molecules25225225.

4. Kumar A, Srivastava R. Rose-like Bi_2WO_6 Nanostructure for Visible-Light-Assisted Oxidation of Lignocellulose-Derived 5-Hydroxymethylfurfural and Vanillyl Alcohol. *ACS Appl Nano Mater* 2021;4:9080-93. DOI: 10.1021/acsanm.1c01679.

5. Yurdakal S, Tek BS, Alagöz O, et al. Photocatalytic Selective Oxidation of 5-(Hydroxymethyl)-2-furaldehyde to 2,5-Furandicarbaldehyde in Water by Using Anatase, Rutile, and Brookite TiO_2 Nanoparticles. *ACS Sustain Chem Eng* 2013;1:456-61. DOI: 10.1021/sc300142a.

6. Zhang Q, Zhang H, Gu B, Tang Q, Cao Q, Fang W. Sunlight-driven photocatalytic oxidation of 5-hydroxymethylfurfural over a cuprous oxide-anatase heterostructure in aqueous phase. *Appl Catal B* 2023;320:122006. DOI: 10.1016/j.apcatb.2022.122006.